TITLE: Increased global functional connectivity correlates with LSD-induced ego-dissolution

AUTHORS

Enzo Tagliazucchi[1,2*], Leor Roseman[3,4], Mendel Kaelen[3], Csaba Orban[3], Suresh Muthukumraswamy[5,6], Kevin Murphy[5], Helmut Laufs[7], Robert Leech[4], John McGonigle[3], Nicolas Crossley[8], Edward Bullmore[9,10,11], Tim Williams[12], Mark Bolstridge[3], Amanda Feilding[13], David Nutt[3] and Robin Carhart-Harris[3*]

ET and LR contributed equally to this work

* Corresponding authors

AFFILIATIONS

[1]Department of Sleep and Cognition, Netherlands Institute for Neuroscience (NIN), an institute of the Royal Netherlands Academy of Arts and Sciences, Amsterdam 1105 BA, the Netherlands.
[2]Institute for Medical Psychology, University of Kiel, Kiel 24113, Germany.
[3]Centre for Neuropsychopharmacology, Department of Medicine, Imperial College London, London W12 0NN, United Kingdom.
[4]Computational, Cognitive and Clinical Neuroscience Laboratory (C3NL), Department of Medicine, Imperial College London, London W12 0NN, United Kingdom.
[5]Cardiff University Brain Research Imaging Centre (CUBRIC), Department of Psychology, Cardiff CF10 3AT, United Kingdom.
[6]Schools of Pharmacy and Psychology, University of Auckland, Auckland 1010, New Zealand.
[7]Neurology Department, Schleswig-Holstein University Hospital, University of Kiel, Kiel 24113, Germany.
[8]Department of Psychosis Studies, Institute of Psychiatry, Psychology and Neurosciences, King's College London, London WC2R 2LS, United Kingdom.
[9]Department of Psychiatry, University of Cambridge, Cambridge CB2 2QQ, United Kingdom.
[10]Cambridgeshire & Peterborough NHS Foundation Trust, Cambridge CB21 5EF, United Kingdom.
[11]GlaxoSmithKline, Alternative Discovery & Development, Brentford TW8 9GS, United Kingdom.
[12]AWP Mental Health NHS Trust, Blackberry Centre, Manor Road, Bristol BS16 2EW, United Kingdom.
[13]The Beckley Foundation, Oxford OX3 9SY, United Kingdom.

CORRESPONDING AUTHORS

Enzo Tagliazucchi
tagliazucchi.enzo@googlemail.com

Robin Carhart-Harris
r.carhart-harris@imperial.ac.uk

SUMMARY (limit = 250 words, currently = 239)

Lysergic acid diethylamide (LSD) is a non-selective serotonin-receptor agonist that was first synthesized in 1938 and identified as (potently) psychoactive in 1943. Psychedelics have been used by indigenous cultures for millennia **[1]**; however, because of LSD's unique potency and the timing of its discovery (coinciding with a period of major discovery in psychopharmacology), it is generally regarded as the quintessential contemporary "psychedelic" **[2]**. LSD has profound modulatory effects on consciousness and was used extensively in psychological research and psychiatric practice in the 1950s and 60s **[3]**. In spite of this, however, there have been no modern human imaging studies on its acute effects on the brain. Here we studied the effects of LSD on intrinsic functional connectivity within the human brain using functional MRI (fMRI). High-level association cortices (partially overlapping with the default mode, salience and frontoparietal attention networks) and the thalamus showed increased global connectivity under the drug. The cortical areas showing increased global connectivity overlapped significantly with a map of serotonin 2A receptor densities (the key site of action of psychedelic drugs **[4]**). LSD also increased global integration by inflating the level of communication between normally distinct brain networks. The increase in global connectivity observed under LSD correlated with subjective reports of ego-dissolution. The present results provide the first evidence that LSD selectively expands global connectivity in the brain, compromising the brain's modular and "rich-club" organization and simultaneously the perceptual boundaries between the self and the environment.

HIGHLIGHTS

- High-level cortical regions and the thalamus show increased global connectivity under LSD.
- The brain's modular and rich-club organization is altered under LSD.
- Increased global connectivity under LSD correlates with ego-dissolution scores.

eTOC Blurb

Tagliazucchi et al. found that increased global communication mediated by the brain's key integration centres underlies the LSD-induced "ego-dissolution" experience. This globally enhanced integration impairs the functional identity of brain systems, leading to feelings of ego-dissolution and disturbed ego-boundaries.

RESULTS

Functional magnetic resonance imaging (fMRI) was used to investigate global and local changes in functional connectivity following intravenous injection of LSD vs. placebo to fifteen healthy volunteers. The experiment followed a randomized and balanced within-subject design and both whole-brain "exploratory" and more selective "hypothesis-driven" data-analysis approaches were employed. Based on the predominantly cortical distribution of 5-HT_{2A} receptors **[5, 6]** (the principal receptor mediating psychedelic effects **[4]**), as well as previous findings with other psychedelics **[5, 7, 8]**, we hypothesised that connectivity changes would implicate high-level cortical networks such as the default-mode network (DMN) **[9]** and salience network **[10]**. The association between these networks and self-consciousness **[7, 11, 12]** led us to expect a parametric correlation with the intensity of subjective reports of ego-dissolution under LSD, i.e. a compromised sense of possessing an integrated and distinct personality or identity.

We first studied changes in the overall connectivity of 401 even-sized regions of interest (ROI) completely covering cortical and sub-cortical grey matter and obtained using a method introduced by Zalesky and colleagues **[13]**. We computed the functional connectivity density (FCD) **[14]** as the average correlation between the spontaneously fluctuating Blood Oxygenation Level Dependent (BOLD) signal at each region of interest and the time series from all remaining ROIs. Thus, high FCD values correspond to regions whose activity is strongly correlated to that of the rest of the brain, whereas activity in regions with low FCD values is weakly correlated to that of the rest of the brain. The average FCDs measured under LSD and placebo are shown in **Figure 1A** as a 3D rendering on top of a grey matter surface. Histograms depicting the distribution of FCD values across all ROIs were obtained for both conditions. In the LSD condition there was a tail of highly coupled regions that was less prominent in the placebo condition (**Figure 1B**). FCD values were globally increased under LSD compared with placebo (inset of **Figure 1B**).

The increases in global connectivity under LSD were observed in predominantly in frontal, parietal and inferior temporal cortices, as well as in the bilateral thalamus. In **Figure 1C** we present a rendering of these effects together with the outline of three resting state networks (RSN) obtained by applying independent component analysis **[15]** to resting state data from 35 healthy subjects in the Human Connectome Project (HCP) data-set (http://www.humanconnectomeproject.org/). These three RSN (bilateral fronto-parietal, default mode and salience networks) showed a significant overlap with FCD increases under LSD (**Figure 1D**) and have been implicated in the action of other psychedelics **[5, 8]**. Additionally, we found a significant overlap between FCD increases under LSD and the distribution of 5-HT_{2A} receptors obtained using PET **[6]** (the key site of action of psychedelic drugs **[4]**), as well as with FCD increases observed under psilocybin (same data and preprocessing as reported in **[16]**) (**Figure 1D**, right). We did not observe significant overlap between FCD increases and the distribution of other serotonin receptors (5-HT_{1A} and 5-HT_{1B}).

Subsequently, we correlated the magnitude of regional FCD increases observed under LSD with the intensity of ego-dissolution reported by the participants (LSD minus placebo) across all regions of interest. Regions surviving correction for multiple comparisons included the bilateral temporo-parietal junction (angular gyrus) and the bilateral insular cortex (red rendering in **Figure 2A**). The specificity of this finding was assessed by also correlating all other VAS scores with FCD increases under LSD. Importantly, ego-dissolution was the only subjective rating that survived this multiple comparisons correction (see **Figure S2** for more information on VAS and ASC scores). In the green rendering in **Figure 2A**, we identify those regions presenting correlations with ego-dissolution scores (corrected for multiple comparisons) and uncorrelated to all other VAS scores (at a level $p<0.05$, uncorrected). Scatter plots of FCD vs. ego-dissolution are shown in **Figure 2B** for four example regions located in the left/right angular gyrus and insula. These regions were selected based on their overlap with the corresponding Automated Anatomical Labeling (AAL) atlas regions, and due to their association with self-awareness **[11, 12, 36, 37]**. Scatter plots of FCD vs. the other five VAS scores are provided in **Figure S4** and plots for four additional regions are provided in **Figure S3**.

The FCD increases indicated that the overall "global" connectivity of the regions in **Figure 1C** increased under LSD relative to placebo. Next, we asked which areas of the brain became especially more engaged with these highly globally connected brain areas under LSD. To do this, we divided the FCD difference map (**Figure 1C**) into four components: a frontal seed (comprising parts of inferior, middle and superior frontal gyri); a parietal seed (bilateral temporo-parietal junction/angular gyrus); the precuneus and the bilateral thalamus. Seed-based regression analyses were subsequently conducted based on each of these four seeds (as the independent variables) with the total 401 ROIs as dependent variables. **Figure 3** displays difference maps with the regions becoming more connected coupled with four FCD-determined seeds (left panel) under LSD relative to placebo. In all four cases, sensory cortices were implicated (right panel). This result was further confirmed by repeating the permutation analysis **[16]** conducted for the FCD map (**Figure 1D**) - yielding a significant overlap between the difference maps and four HCP-derived RSNs: a sensorimotor RSN spanning the pre- and post-central gyri, two visual RSN (medial and lateral) and an auditory RSN encompassing the superior temporal cortex (including the primary auditory cortex in the Heschl's gyrus). For comparison, the contour of these RSN is overlaid with the maps of statistically significant regions in **Figure 3** (right panel).

Next, we evaluated whether LSD only scaled the magnitude of the coupling or also re-arranged connectivity patterns in the brain, independently of the coupling strength. To do this, we studied the modularity of whole-brain functional connectivity networks having the ROIs as nodes. In the present context, modularity measures how well the brain can be parcellated into modules having dense within-module and sparse between-module connectivity **[17]**. Based on the observation of increased between-network connectivity under LSD (**Figure 3**), as well as previous findings with other psychedelics **[18]**, we predicted that there would be a decrease in brain modularity under the drug, indicating a reduction in the separation of intrinsic brain networks. As shown in **Figure 4A**, this prediction was supported over an extended range of functional network link densities (ratio of the

number of binary connections present in the network to the maximum possible number of connections; see methods). In **Figure 4B**, we show the modules identified by the modularity optimization algorithm. We also computed the participation coefficient of each node (measuring how much each node communicates across modules relative to how much they communicate within their own module **[17]**) and observed increased participation coefficients in frontal and midline regions (**Figure 4C**) overlapping with those in Figure. 1C, suggesting that these areas serve as conduits for increased between-module communication under LSD.

Finally, we investigated changes in the level of integration between highly coupled regions by means of the so called "rich club" coefficient $\Phi(k)$. This metric calculates the ratio of links between nodes of degree (i.e. number of attached links) higher than a certain number (k) over the maximum possible number of links between them, and it is normalized by the same metric computed after degree-preserving randomization of the network **[19]**. In **Figure 4D** we show that the rich club coefficient is higher under placebo than LSD, indicating that LSD decreases the level of (preferential) communication between the brain's dominant hub regions. These hub regions are found within a single module (corresponding to primary sensory areas, green module in **Figure 4B**) as revealed by the k-core of the LSD and placebo networks (with k=100), defined as the smallest subset of nodes with degree at least equal to k (see **Figure 4E**). Thus, LSD enhances between-module integration at the expense of impairing within-module communication of highly coupled nodes.

DISCUSSION

Taken together, the present results indicate that LSD enhances global and between-module communication while diminishing the integrity of individual modules and that this effect is mediated by the brain's key integration centres such as those that are rich in serotonin 2A receptors. These results invite comparisons with those of our previous functional imaging studies with psilocybin, a related compound and another serotonergic psychedelic. For example, in **[5]** we reported decreases in functional connectivity between anterior and posterior nodes of the DMN under psilocybin, and in Carhart-Harris et al., 2014 **[20]** and Muthukumaraswamy et al., 2013 **[21]** we suggested that decreased within-network integrity was a general property of psychedelics. Furthermore, two subsequent reports detailed increased between-RSN connectivity under psilocybin **[18, 22]**, matching the directionality of the effects found here with LSD. Indeed, re-analysis of our previously-acquired psilocybin fMRI data revealed FCD increases in regions similar to those observed here with LSD (**Figures 1D** and **S1**). Importantly, despite overlap with the default mode, frontoparietal and salience networks, the results of the current FCD analysis were not constrained a priori to these or any other specific RSN.

Intriguingly, a formal analysis revealed significant overlap between the regions of increased global connectivity under LSD and those that express the serotonin 2A receptors in especially high concentrations. Serotonin 2A receptor agonism is known to increase cell excitability (in particular that of layer V pyramidal neurons) **[23]**, which may result in higher metabolic demands. Increased glucose

metabolism in frontal, temporal and subcortical regions was reported for serotonergic psychedelics and these increases correlated with subjective reports of ego-dissolution **[24]**. Glucose metabolism is also known to covariate with the density of functional connections **[25]**, thus establishing a possible connection between the FCD increases observed here and 5-HT_{2A}-mediated changes in neural excitability.

Electroencephalography studies performed during the 1950s and 1960s reported broadband decreases in oscillatory power under LSD **[26]** and magnetoencephalography recently revealed diminished power in a broad range of frequency bands after psilocybin infusion **[21]**. Serotonin 2A receptor-mediated oscillatory desynchronization can be traced to an uncoupling of layer 5 pyramidal cell firing from local field potential oscillations **[27]** – suggesting that dysregulating the firing of these neurons is critical. In the human cortex, decreases in alpha power after psilocybin infusion were particularly marked and decreased alpha in the posterior DMN (precuneus/posterior cingulate cortex) correlated with the intensity of ego-dissolution **[20]**. A number of multimodal EEG-fMRI studies have now revealed an inverse correlation between global functional connectivity and power in the alpha band **[28, 29, 30]**, which reconciles these electrophysiological observations with our findings of increased global connectivity in high-level association areas with both LSD and psilocybin. Alpha oscillations have been hypothesized to inhibit or regulate task-irrelevant (i.e. "spontaneous" or "on-going") neural processes **[31]**; thus, findings of reduced-alpha under psychedelics suggest that these drugs could reduce this inhibition (i.e. be "disinhibitory"). It must be noted, however, that alpha oscillations are linked to a number of cognitive processes (e.g. attention, memory, executive control and conscious access) **[32]** and the hypothesised "disinhibition" cannot be directly inferred from the present results.

The areas of the brain that displayed increased global connectivity under LSD have different functional roles. The fronto-parietal cortex is implicated in conscious information access **[33]** and its activity is suppressed in some states of diminished conscious awareness (such as seizures or deep sleep) **[34]**, even though an unequivocal link between fronto-parietal activity and the conscious state is lacking. Different DMN components perform functions related to self-consciousness: activity in the precuneus correlates with self-reflection processes and autobiographical memory retrieval **[35]**, while the activation of temporo-parietal junctions is typical of out-of-body experiences **[36]**. The bilateral insular cortex is related to self-awareness **[37]**, as well as to the processing of emotional information **[38]**, that could also play an important role in the psychedelic experience. One intriguing possibility is that increased cross talk between these networks and other brain systems underlies the experience of ego-dissolution under LSD. This scenario is supported by our observation of positive correlations between increased FCD in the bilateral temporo-parietal junction and insular cortex and subjective reports of ego-dissolution. Furthermore, we observed that the increases in global connectivity in these high-level regions particularly involved sensory areas. This increased communication between high-level (association) and lower-level (sensory) cortices might represent a collapse in the normal hierarchical organization of the brain **[20]** such that the boundaries between lower level systems anchored to the external world and higher level systems operating more autonomously from sensory

information, become blurred. It is intriguing to speculate whether this blurring of boundaries and putative expansion of the "global workspace" **[33]** are related to the blurring of ego-boundaries and the experiences of ego-dissolution and "expanded awareness" reported in relation to psychedelics.

It is deserving of mention that our exploratory imaging analysis revealed significant (corrected) correlations with only one (out of 6) VAS items, i.e. the one that enquired about feelings of ego-dissolution. That the results of these exploratory, whole-brain analyses correlated selectively with ego-dissolution may be significant, as it suggests that this phenomenon is important **[7]** and dependent on changes that implicate the whole of the brain rather than specific functional modules. It remains possible however that other aspects of the psychedelic experience (e.g. visual hallucinations) may depend on changes in the functioning of a particular module (e.g. the visual cortex) and this is something we intend to investigate in the future.

As mentioned above, the quality of consciousness under psychedelics is frequently referred to as "expanded" **[20]**. It is reasonable to infer therefore, that the neurophysiology of the psychedelic state will contrast with that of states of "diminished consciousness", such as deep sleep or under general anesthesia. Our results support this inference on many levels. As discussed above, increased fronto-parietal FCD under LSD suggests higher metabolism in these regions, whereas unconscious states are generally characterized by diminished fronto-parietal metabolism and connectivity **[34]**. Deep sleep, for instance, presents decreased density and efficiency of fronto-parietal functional connections **[39]**. Both sleep and anesthesia are characterized by a breakdown of functional integration, resulting in increased modularity values **[40, 41]**, whereas we observed decreased modularity values under LSD, reflecting enhanced between-module cross-talk. Broadly speaking, this study's results are consistent with the previous hypothesis that the psychedelic and unconscious states occupy polar-opposite ends of a spectrum of conscious states, defined by their level of entropy or randomness **[20]**. This hypothesis can now be updated to state that the brain's level of modularity (low modularity being characteristic of random and disordered networks **[17]**), during a particular period of time (e.g. the duration of resting-state scan), is predictive of the subjective quality of consciousness that is experienced during that period. Further work is required to develop our characterization and subsequent quantification of the subjective nature of conscious states **[42]**; however, the present measure of ego-dissolution can be viewed as a start in this direction.

Some limitations of our study must be acknowledged. First, while we attempted by all available means to reduce the impact of head motion in our results and to show that our results cannot be attributed to motion confounds (see "Motion" section in the supplemental experimental procedures), significant differences in head motion persisted between conditions. Second, the particularly strict criteria used to combat motion artefacts reduced our original sample of 20 subjects to a smaller sample of 15 "clean" datasets. Third, our analysis of ego-dissolution was based on a single numerical report by experienced psychedelic drug users; future studies should attempt a more thorough characterization of the subjective dimension of this experience. Finally, since the participants were experienced psychedelic drug users it is more likely they could differentiate the LSD from the placebo, potentially

leading to demand characteristics. It would be interesting to repeat these analyses in psychedelic-naïve participants to test whether past-use of psychedelics can be predictive of the reported effects, although we failed to observe any correlations between past-use and the above-reported effects of LSD in the present study.

In conclusion, the present study aimed to explore one of the most remarkable and least understood domains of the psychedelic experience, known both colloquially and academically as "ego-dissolution". It revealed an increase in global integration within the brain (but a decrease in within-module integrity), seemingly mediated by high-level cortical association regions that are rich in serotonin 2A receptors as well as the thalamus. Importantly, the increases in global integration in cortical association regions selectively correlated with subjective ratings of ego-dissolution. These results help to inform not just on the neurobiology of the psychedelic experience but on a fundamental aspect of human consciousness, namely the sense of possessing a coherent "self" or "ego" that is distinct from others and separate from the external environment. Further work is required to develop these insights and explore other interesting aspects of the phenomenology of the psychedelic experience. Finally, the present study reinforces the view that, conducted with appropriate care, human research with psychedelic drugs is safe and can provide valuable insights in human neuroscience.

EXPERIMENTAL PROCEDURES

The experimental procedures (including information on subject recruitment, experimental design, data acquisition and data analysis) are provided in the supplemental information.

AUTHOR CONTRIBUTIONS

ET analyzed the data, produced all figures and wrote the paper. LR contributed to study design, analyzed the data and wrote the paper. MK contributed to study design, recruitment of volunteers and data analysis. CO contributed to data analysis. SDM contributed to study design and coordination. KM contributed to data analysis. HL contributed to data analysis and edited the paper. RL contributed to study design and edited the paper. JM contributed to data analysis. NC and EB contributed to data analysis and edited the paper. TW and MB helped perform the research, care for the participants, administered the LSD and served as medical/psychiatric cover for the study. AF was instrumental in initiating the research and edited the paper. DJN advised on the study's design and implementation and edited the paper. RCH designed and led the study, oversaw recruitment, contributed to data analysis and edited the paper.

ACKNOWLEDGMENTS

This research received financial support from the Safra Foundation (who fund DJN as the Edmond J. Safra Professor of Neuropsychopharmacology) and the Beckley Foundation (it was conducted as part of the Beckley-Imperial research programme). ET is supported by a postdoctoral fellowship of the AXA Research Fund. RCH is supported by an MRC clinical development scheme grant. SDM is supported by a Royal Society of New Zealand Rutherford Discovery Fellowship. KM is supported by a Wellcome Trust Fellowship (WT090199). The researchers would like to thank supporters of the Walacea.com crowd-funding campaign for helping to secure the funds required to complete the study. This report presents independent research carried out at the NIHR/Wellcome Trust Imperial Clinical Research Facility. Authors declare no conflict of interest.

REFERENCES

1. Metzner, R. (1998) Hallucinogenic drugs and plants in psychotherapy and shamanism. J Psychoactive Drugs 30(4),333-341.

2. Hofmann, A. (1980) LSD : my problem child. McGraw-Hill.

3. Grob, C. (1996) Psychiatric research with hallucinogens- what have we learned?. VWB, Verlag für Wissenschaft und Bildung.

4. Glennon, R.A., Titeler, M., McKenney, J.D. (1984) Evidence for 5-HT 2 involvement in the mechanism of action of hallucinogenic agents. Life sciences 35(25), 2505-2511.

5. Carhart-Harris, R. L., Erritzoe, D., Williams, T., Stone, J. M., Reed, L. J., Colasanti, A., Tyacke, R.J., Leech, R., Malizia, A.L., Murphy, K., Hobden, P., Evans, J., Feilding, A., Wise, R.G., Nutt, D. J. (2012) Neural correlates of the psychedelic state as determined by fMRI studies with psilocybin. Proc. Acad. Sci. USA 109(6), 2138-2143.

6. Saulin, A., Savli, M., Lanzenberger, R. (2012) Serotonin and molecular neuroimaging in humans using PET. Amino acids, 42(6), 2039-2057.

7. Lebedev, A. V., Lövdén, M., Rosenthal, G., Feilding, A., Nutt, D. J., Carhart- Harris, R. L. (2015) Finding the self by losing the self: Neural correlates of ego- dissolution under psilocybin. Hum. Brain Mapp. 36, 3137–3153.

8. Palhano-Fontes, F., Andrade, K. C., Tofoli, L. F., Santos, A. C., Crippa, J. A. S., Hallak, J. E., Ribeiro, S., de Araujo, D. B. (2015) The psychedelic state induced by ayahuasca modulates the activity and connectivity of the default mode network.PloS one 10, e0118143.

9. Raichle, M. E., MacLeod, A. M., Snyder, A. Z., Powers, W. J., Gusnard, D. A., & Shulman, G. L. (2001) A default mode of brain function. Proc. Natl. Acad. Sci. USA 98(2), 676-682.

10. Seeley, W. W., Menon, V., Schatzberg, A. F., Keller, J., Glover, G. H., Kenna, H., Reiss, A.L., Greicius, M. D. (2007). Dissociable intrinsic connectivity networks for salience processing and executive control. J. Neurosci. 27(9), 2349-2356.

11. Vogeley, K., May, M., Ritzl, A., Falkai, P., Zilles, K., Fink, G.R. (2004) Neural correlates of first-person perspective as one constituent of human self-consciousness. J. Cogn. Neurosci. 16(5), 817-827.

12. Carhart-Harris, R.L., Friston, K.J. (2010) The default-mode, ego-functions and free-energy: a neurobiological account of Freudian ideas. Brain, awq010.

13. Zalesky, A., Fornito, A., Harding, I. H., Cocchi, L., Yücel, M., Pantelis, C., Bullmore, E. T. (2010) Whole-brain anatomical networks: does the choice of nodes matter?. *Neuroimage 50*(3), 970-983.

14. Tomasi, D., Volkow, N.D. (2010) Functional connectivity density mapping. Proc. Natl. Acad. Sci. USA 07(21), 9885-9890.

15. Beckmann, C. F., DeLuca, M., Devlin, J. T., & Smith, S. M. (2005) Investigations into resting-state connectivity using independent component analysis. Phil. Trans. Roy. Soc. B 360(1457), 1001-1013.

16. Tagliazucchi, E., Carhart-Harris, R., Leech, R., Nutt, D., Chialvo, D.R. (2014) Enhanced repertoire of brain dynamical states during the psychedelic experience. Hum. Brain Mapp. 35(11), 5442-5456.

17. Bullmore, E., Sporns, O. (2009) Complex brain networks: graph theoretical analysis of structural and functional systems. Nat. Rev. Neurosci. 10(3), 186-198.

18. Roseman, L., Leech, R., Feilding, A., Nutt, D.J., Carhart-Harris, R.L. (2014) The effects of psilocybin and MDMA on between-network resting state functional connectivity in healthy volunteers. Front. Hum. Neurosci 8.

19. van den Heuvel, M. P., Sporns, O. (2011) Rich-club organization of the human connectome. J. Neurosci. 31(44), 15775-15786.

20. Carhart-Harris, R. L., Leech, R., Hellyer, P. J., Shanahan, M., Feilding, A., Tagliazucchi, E., Chialvo, D.R., Nutt, D. (2014) The entropic brain: a theory of conscious states informed by neuroimaging research with psychedelic drugs. Front. Hum. Neurosci. 8.

21. Muthukumaraswamy, S. D., Carhart-Harris, R. L., Moran, R. J., Brookes, M. J., Williams, T. M., Errtizoe, D., Sessa, B., Papadopoulos, A., Bolstridge, M., Singh, K.D., Feilding, A., Friston, K.J., Nutt, D. J. (2013) Broadband cortical desynchronization underlies the human psychedelic state. J. Neurosci 33(38), 15171-15183.

22. Carhart-Harris, R. L., Leech, R., Erritzoe, D., Williams, T. M., Stone, J. M., Evans, J., Sharp, D.J., Feilding, A., Wise, R.G., Nutt, D. J. (2013) Functional connectivity measures after psilocybin inform a novel hypothesis of early psychosis. Schiz. Bull. 39(6), 1343-1351.

23. Andrade, R. (2011) Serotonergic regulation of neuronal excitability in the prefrontal cortex. Neuropharmacology 61(3), 382-386.

24. Vollenweider, F. X., Leenders, K. L., Scharfetter, C., Maguire, P., Stadelmann, O., Angst, J. (1997) Positron emission tomography and fluorodeoxyglucose studies of metabolic hyperfrontality and psychopathology in the psilocybin model of psychosis. Neuropsychopharmacology 16(5), 357-372.

25. Tomasi, D., Wang, G.J., Volkow, N.D. (2013) Energetic cost of brain functional connectivity. Proc. Natl. Acad. Sci. USA 110(33), 13642-13647.

26. Fink, M. (1969) EEG and human psychopharmacology. Ann. Rev. Pharmacol. 9(1), 241-258.

27. Celada, P., Puig, M. V., Díaz-Mataix, L., Artigas, F. (2008) The hallucinogen DOI reduces low-frequency oscillations in rat prefrontal cortex: reversal by antipsychotic drugs. Biol. Psych. *64*(5), 392-400.

28. Scheeringa, R., Petersson, K. M., Kleinschmidt, A., Jensen, O., Bastiaansen, M. C. (2012) EEG alpha power modulation of FMRI resting-state connectivity. Brain Conn. 2(5), 254-264.

29. Tagliazucchi, E., Von Wegner, F., Morzelewski, A., Brodbeck, V., Laufs, H. (2012) Dynamic BOLD functional connectivity in humans and its electrophysiological correlates. Front. Hum. Neurosci. 6.

30. Chang, C., Liu, Z., Chen, M. C., Liu, X., Duyn, J. H. (2013) EEG correlates of time-varying BOLD functional connectivity. Neuroimage 72, 227-236.

31. Klimesch, W., Sauseng, P., Hanslmayr, S. (2007) EEG alpha oscillations: the inhibition-timing hypothesis. Brain Res. Rev. 53(1), 63-88.

32. Bazanova, O. M., Vernon, D. (2014) Interpreting EEG alpha activity. Neurosci. & Behav. Rev. 44, 94-110.

33. Dehaene, S., Naccache, L. (2001) Towards a cognitive neuroscience of consciousness: basic evidence and a workspace framework. Cognition 79(1), 1-37.

34. Boly, M., Phillips, C., Tshibanda, L., Vanhaudenhuyse, A., Schabus, M., Dang- Vu, T. T., Moonen, G., Hustinx, R., Maquet, P., Laureys, S. (2008) Intrinsic brain activity in altered states of consciousness. Ann. NY Acad. Sci. 1129(1), 119-129.

35 . Johnson, S. C., Baxter, L. C., Wilder, L. S., Pipe, J. G., Heiserman, J. E., Prigatano, G. P. (2002) Neural correlates of self- reflection. Brain, 125(8), 1808-1814.

36. Blanke, O., Ortigue, S., Landis, T., Seeck, M. (2002) Neuropsychology: Stimulating illusory own-body perceptions. Nature 419(6904), 269-270.

37. Craig, A.D. (2011) Significance of the insula for the evolution of human awareness of feelings from the body. Ann. NY Acad. Sci. 1225, 72-82.

38. Phan, K. L., Wager, T., Taylor, S. F., Liberzon, I. (2002) Functional neuroanatomy of emotion: a meta-analysis of emotion activation studies in PET and fMRI. Neuroimage 16(2), 331-348.

39. Uehara, T., Yamasaki, T., Okamoto, T., Koike, T., Kan, S., Miyauchi, S., Kira, J., Tobimatsu, S. (2014) Efficiency of a “small-world” brain network depends on consciousness level: a resting-state FMRI study. Cereb. Cortex 24(6), 1529-1539.

40. Tagliazucchi, E., Von Wegner, F., Morzelewski, A., Brodbeck, V., Borisov, S., Jahnke, K., & Laufs, H. (2013) Large-scale brain functional modularity is reflected in slow electroencephalographic rhythms across the human non-rapid eye movement sleep cycle. Neuroimage, 70, 327-339.

41. Schrouff, J., Perlbarg, V., Boly, M., Marrelec, G., Boveroux, P., Vanhaudenhuyse, A., Bruno, M.A., Laureys, S., Phillips, C., Pélégrini-Isaac, M., Maquet, P., Benali, H. (2011) Brain functional integration decreases during propofol-induced loss of consciousness. Neuroimage 57(1), 198-205.

42. Studerus, E., Gamma, A., Vollenweider, F.X. (2010) Psychometric evaluation of the altered states of consciousness rating scale (OAV). PLoS One 5(8) e12412-e12412.

FIGURE CAPTIONS

Figure 1. LSD selectively increases global functional connectivity of higher-level integrative cortical and sub-cortical regions. (A) Average FCD under the placebo and LSD conditions. (B) Normalized histogram (P) of all FCD values for both conditions (mean ± SEM). The inset shows the whole-brain FCD averages (*p<0.05, two-tailed t-test). (C) Rendering of significant FCD increases under LSD vs. placebo (thresholded at p<0.05, two-tailed t-test, FDR-controlled for multiple comparisons). Outlines of the bilateral fronto-parietal, salience and default-mode RSN are overlaid on top of the map of FCD significant increases. (D) Quantitative analysis of the overlap between significant FCD increases and eight RSN obtained from 35 subjects scanned in the Human Connectome Project (*FP*=fronto-parietal, *Sal*=salience, *DMN*=default mode, *Vis L*=lateral visual, *Aud*=auditory, *Vis M*=medial visual, *SM*=sensorimotor), as well as 5-HT_{2A} receptor concentration and FCD increases under psilocybin. Only *FP*, *DMN*, *Sal*, and the maps of 5-HT_{2A} concentration and FCD increases under psilocybin had an overlap significantly higher than the one observed when spatially randomizing the networks (mean ± SD, *p<0.05, Bonferroni corrected for multiple comparisons). For a description of the randomization procedure see **[16]** and the Supp. Info.

Figure 2. FCD increases correlate with subjective reports of ego-dissolution. (A) Brain regions where a significant (p<0.05, two-tailed, FDR-controlled for multiple comparisons) correlation between FCD and subjective reports of ego-dissolution (LSD minus placebo) was found are colored in red. Brain regions where none of the other VAS scores correlated with FCD at p<0.05, two-tailed, uncorrected (i.e. regions presenting the most selective correlations between FCD increases and ego-dissolution scores) are colored in green. (B) Association between FCD increases and reports of ego-dissolution in four example ROIs (bilateral angular gyrus and insular cortex).

Figure 3. LSD increases between-system functional connectivity. Results of seed correlation analyses based on four ROIs (left panel) defined from the map of significant FCD increases (Figure 1C). In the right panel, regions in red indicate significantly higher connectivity (p<0.05, two-tailed t-test, FDR-controlled for multiple comparisons) with the seed (first column, in blue) under LSD relative to the placebo. A permutation test revealed that only four RSN present a significant (p<0.05, Bonferroni corrected for multiple comparisons) overlap with the functional connectivity increases under LSD: the sensorimotor (SM), auditory (Aud), visual medial (Vis M) and visual lateral (Vis L) RSNs. The contour of these RSN is jointly rendered with the maps of functional connectivity changes.

Figure 4. LSD increases global integration. (A) Modularity vs. link density for the LSD and placebo conditions (mean ± SEM, *p<0.05, two-tailed t-test, FDR-controlled for multiple comparisons). The inset shows the same for networks after degree-preserving randomization (no significant differences were found). (B) Rendering of the modules identified at a reference link density of 0.3, for the placebo (up) and LSD (bottom) conditions. (C) Regions presenting increased participation coefficient in LSD vs. placebo (link density = 0.3, p<0.05 two-tailed t-test, FDR-controlled for multiple comparisons). (D)

Normalized rich club coefficient $\phi(k)$ for LSD and placebo; the inset shows the difference between both conditions (mean $\pm$ SEM, link density = 0.3, *p<0.05, two-tailed t-test, FDR-controlled for multiple comparisons). (E) k-cores (k = 100) for placebo (up) and LSD (bottom) conditions.

Figure

Click here to download Figure fig1.jpg

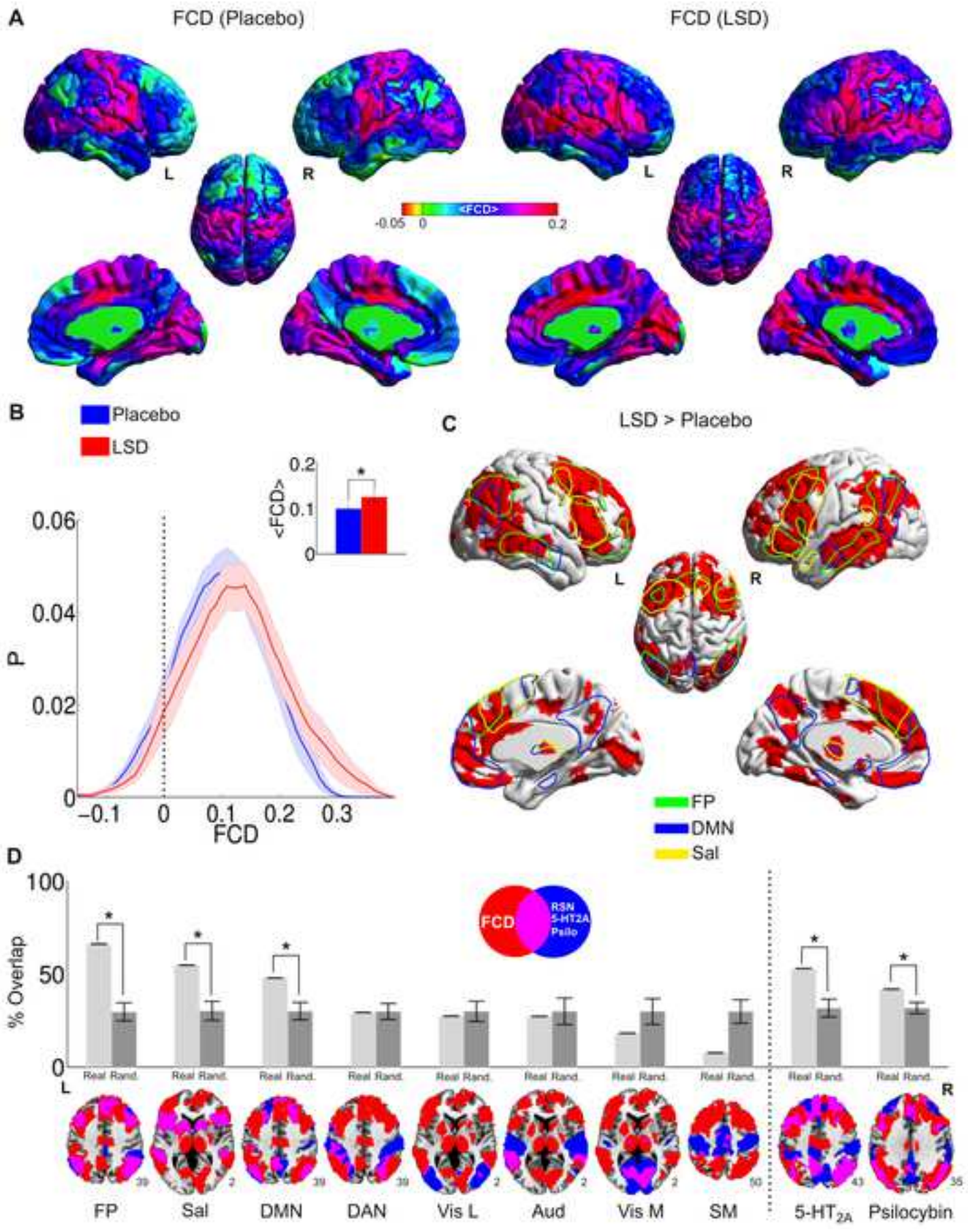

Figure

Click here to download Figure fig2.jpg

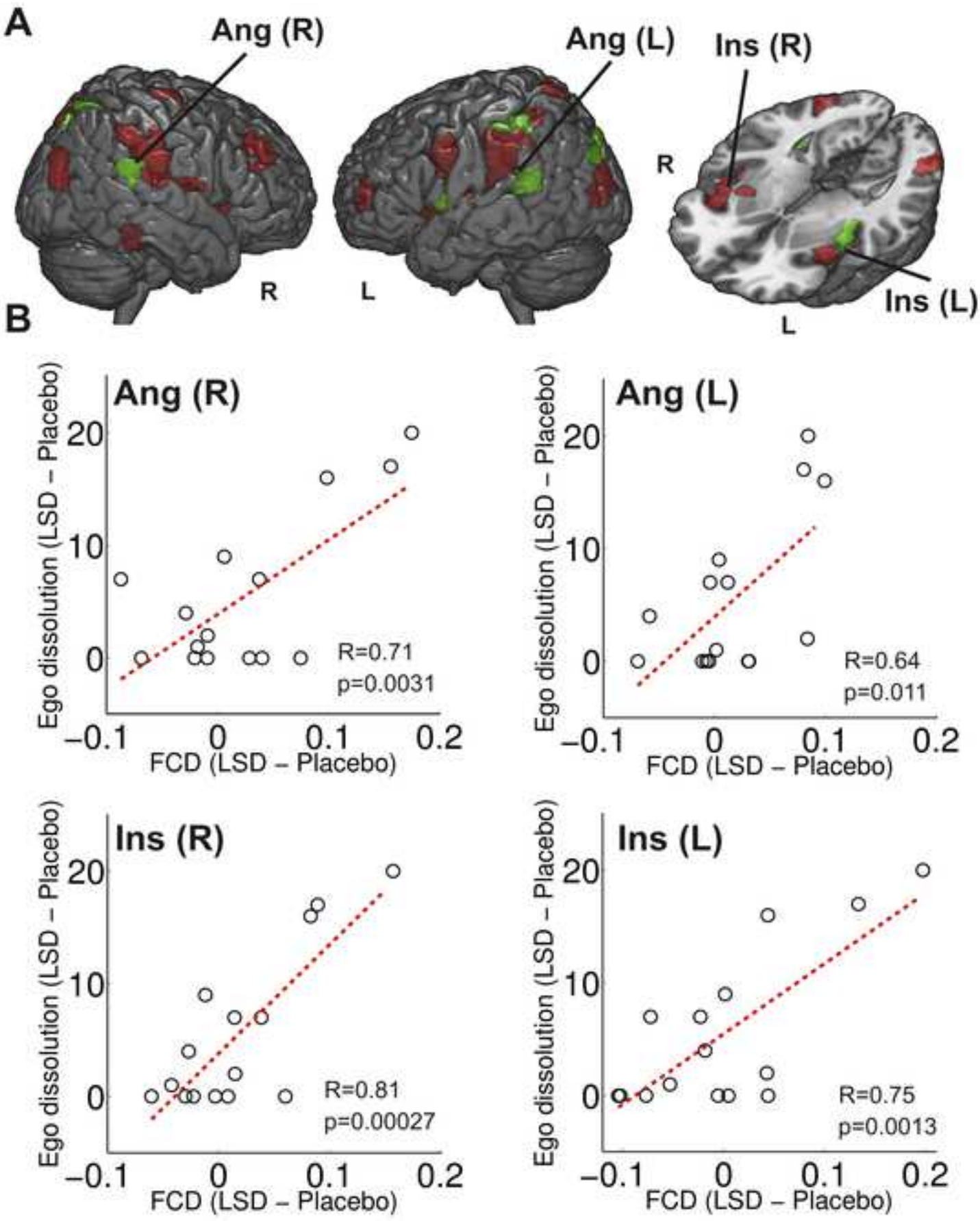

Figure

Click here to download Figure fig3.jpg

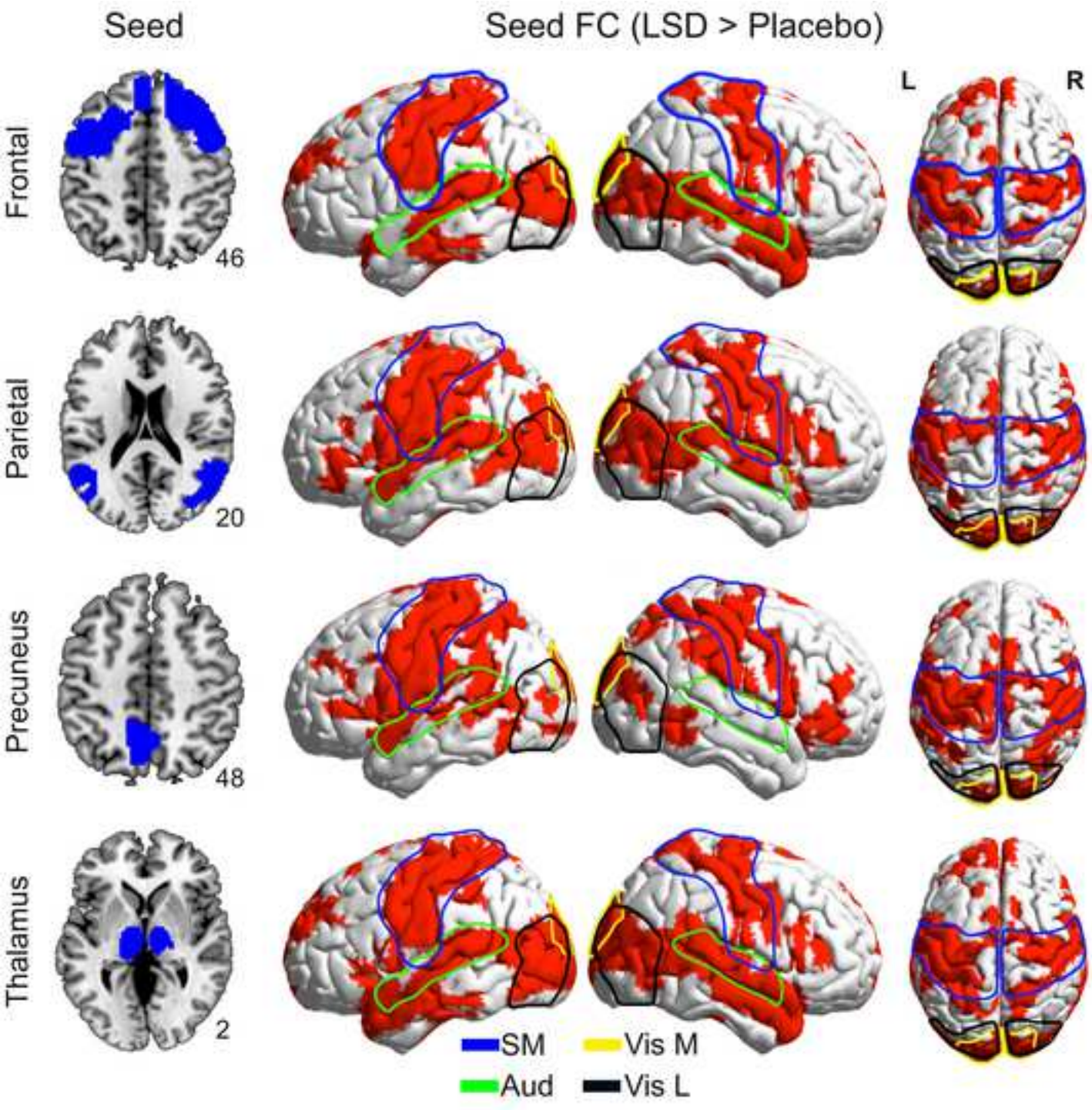

Figure

Click here to download Figure fig4.jpg

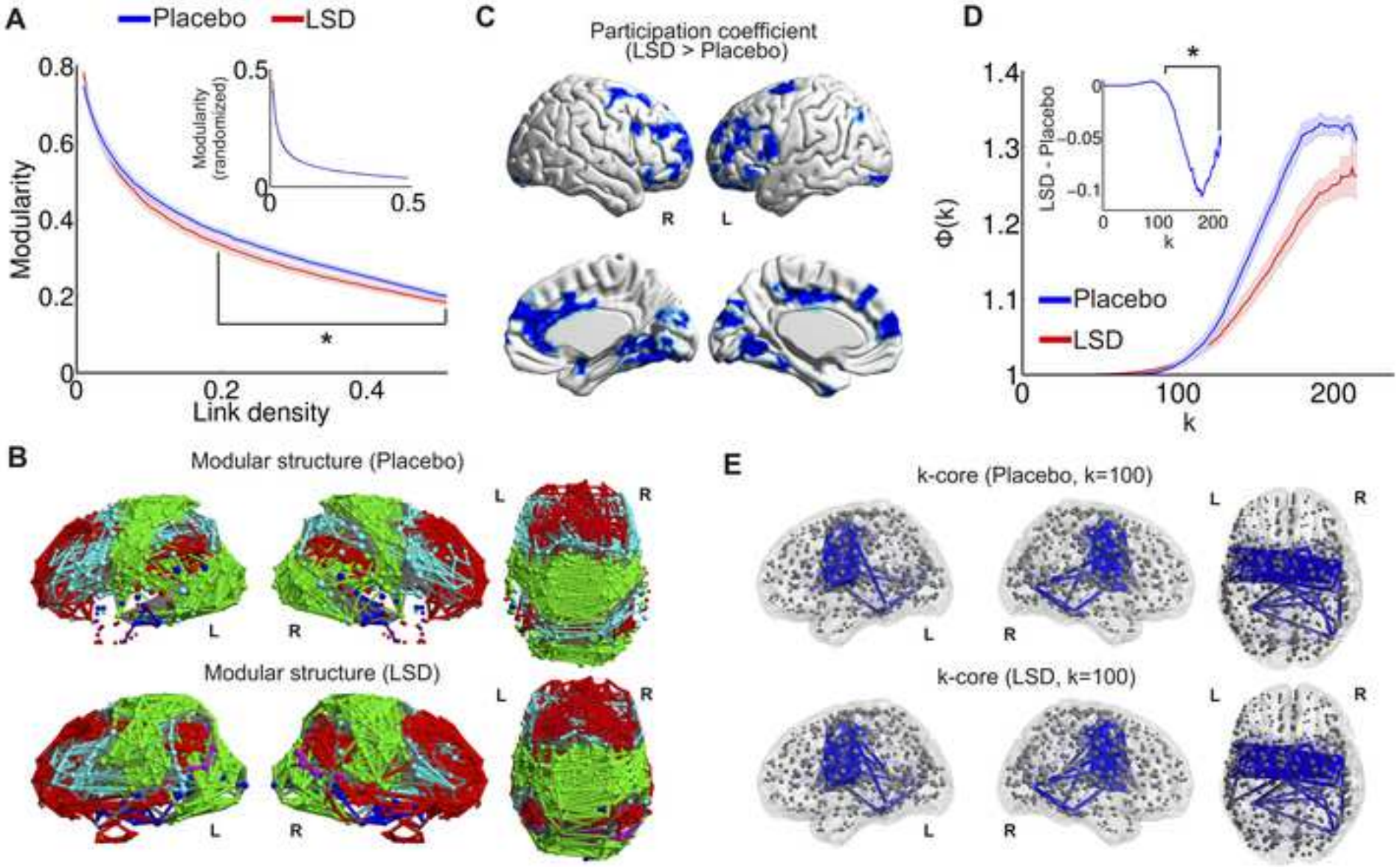

Supplemental Figures and Legends

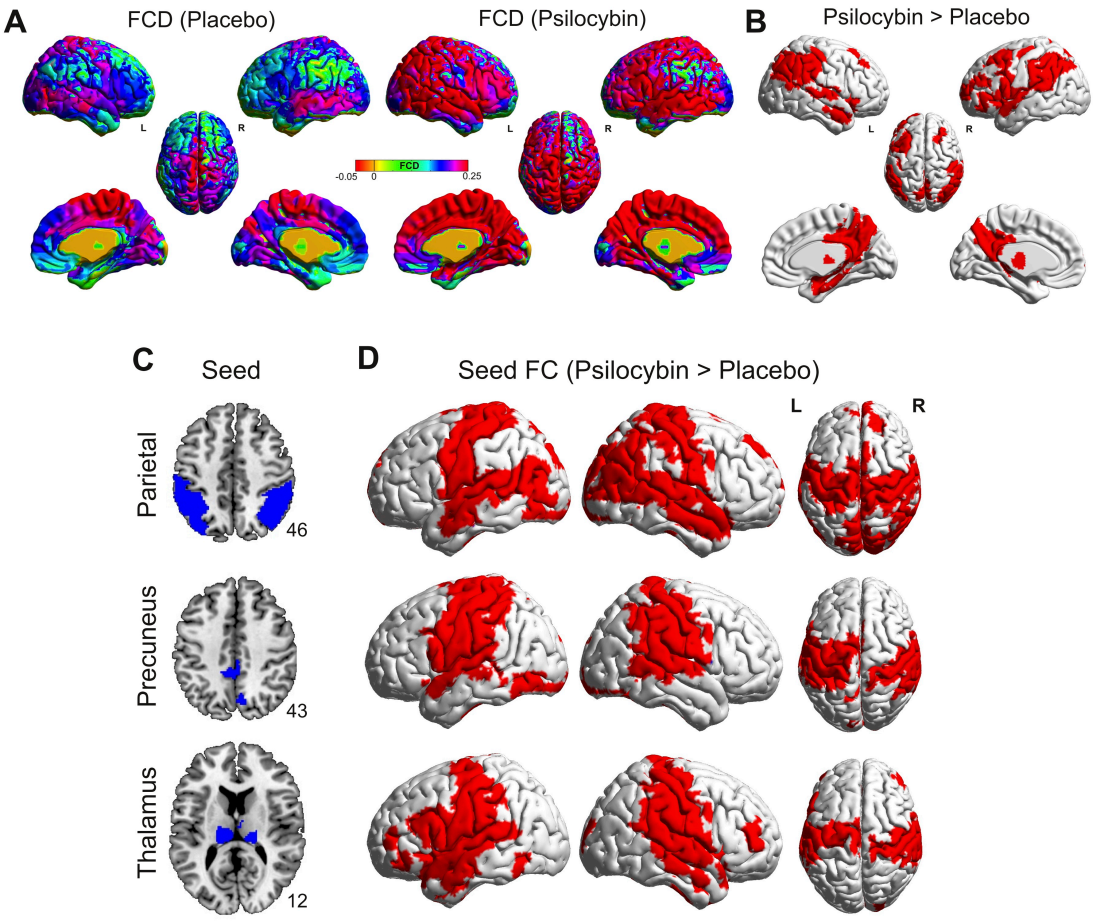

Figure S1: Psilocybin selectively increases global functional connectivity of higher-level integrative cortical and sub-cortical regions, and increases between-system functional connectivity. (A) Average FCD under the placebo and psilocybin conditions. (B) Rendering of significant FCD increases under psilocybin vs. placebo (thresholded at $p<0.05$, FDR-controlled for multiple comparisons). Subjects and data preprocessing is as reported in Tagliazucchi et al., 2014. (C) Regions for seed correlation analysis (defined from the map of FCD increases in Panel B). (D) Results of seed correlation. Regions in red present significantly higher connectivity ($p<0.05$, FDR-controlled for multiple comparisons) with the seeds (panel C) under psilocybin compared with placebo. Subjects and data preprocessing is as reported in [S1].

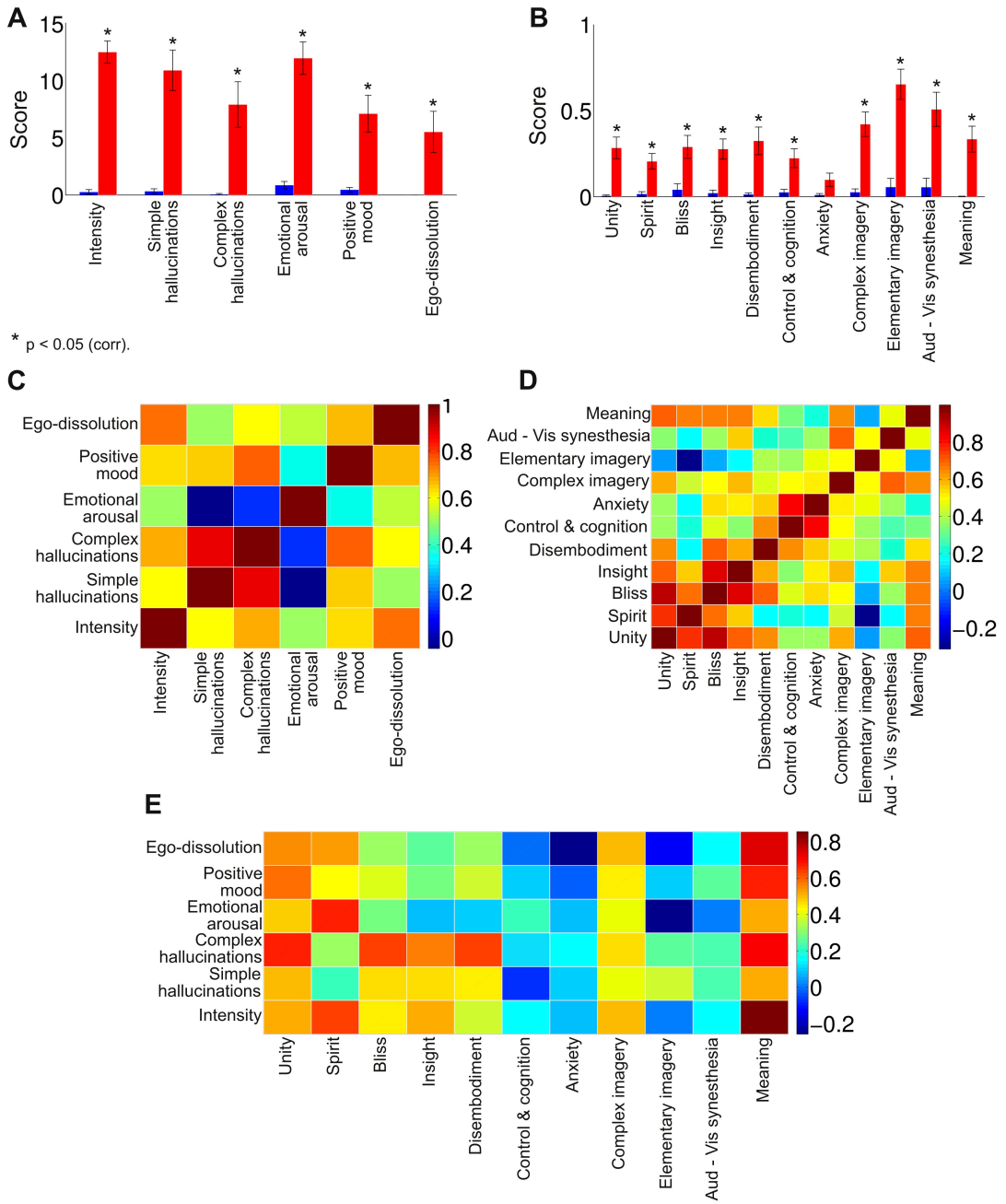

Figure S2: (A) Average VAS scores for LSD (red) and placebo (blue) (mean ± SEM). (B) Average ASC scores for LSD (red) and placebo (blue) (mean ± SEM). Significance tested with the nonparametric Wilcoxon's signed-rank test, Bonferroni correction for multiple comparisons applied. (C) Correlation between VAS scores across participants. (D) Correlation between ASC scores across participants. (E) Correlation between VAS scores and ASC scores across participants. For the full description of the VAS and ASC items see the corresponding subsections in the Supplemental Experimental Procedures.

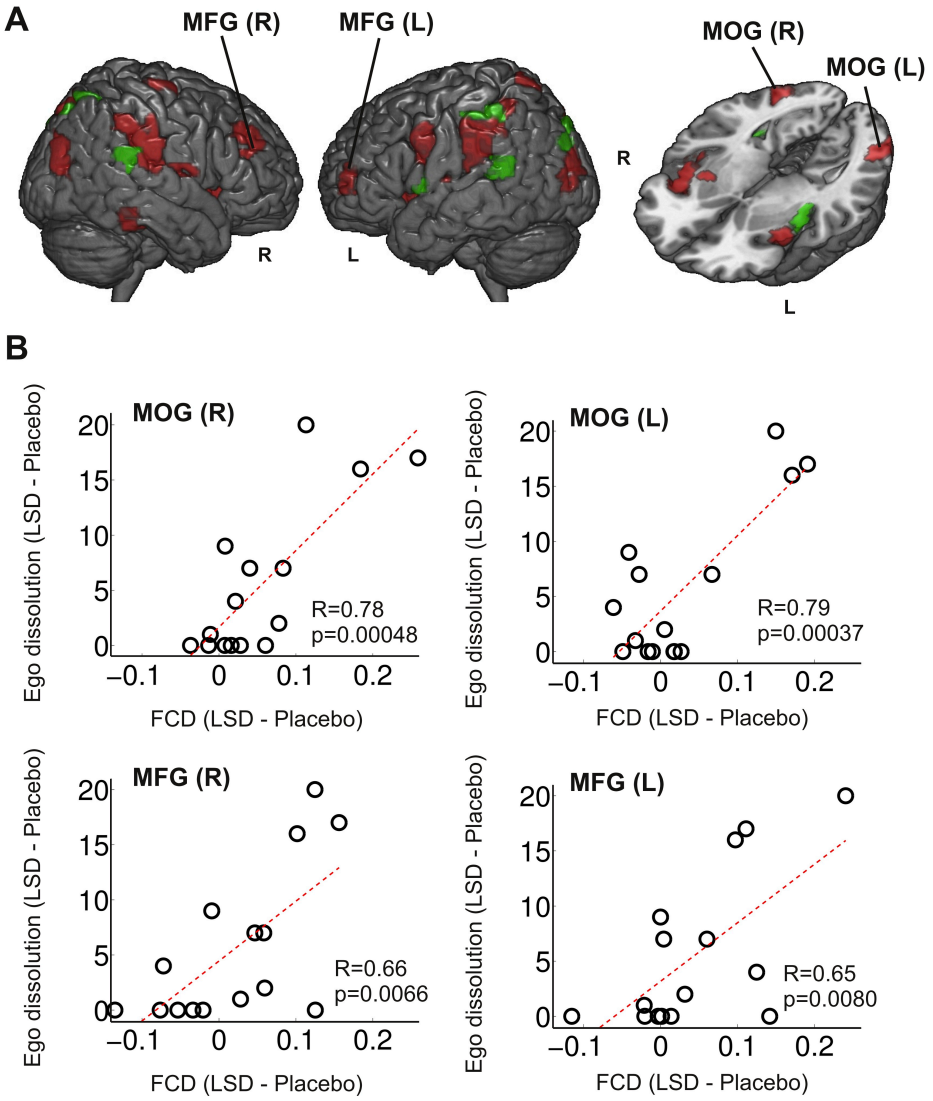

Figure S3: (A) Regions where a significant correlation between FCD increases and ego-dissolution scores was observed under LSD ($p<0.05$, FDR-corrected for multiple comparisons). For a description of the colour scheme, see the analogous Figure 2A in the manuscript text. (B) Scatter plots of ego-dissolution changes under LSD (minus placebo) vs. FCD increases for four additional regions: left/right middle frontal gyrus (MFG) and left/right middle occipital gyrus (MOG). In the inset, Pearson's R and the associated (uncorrected) p-values are provided.

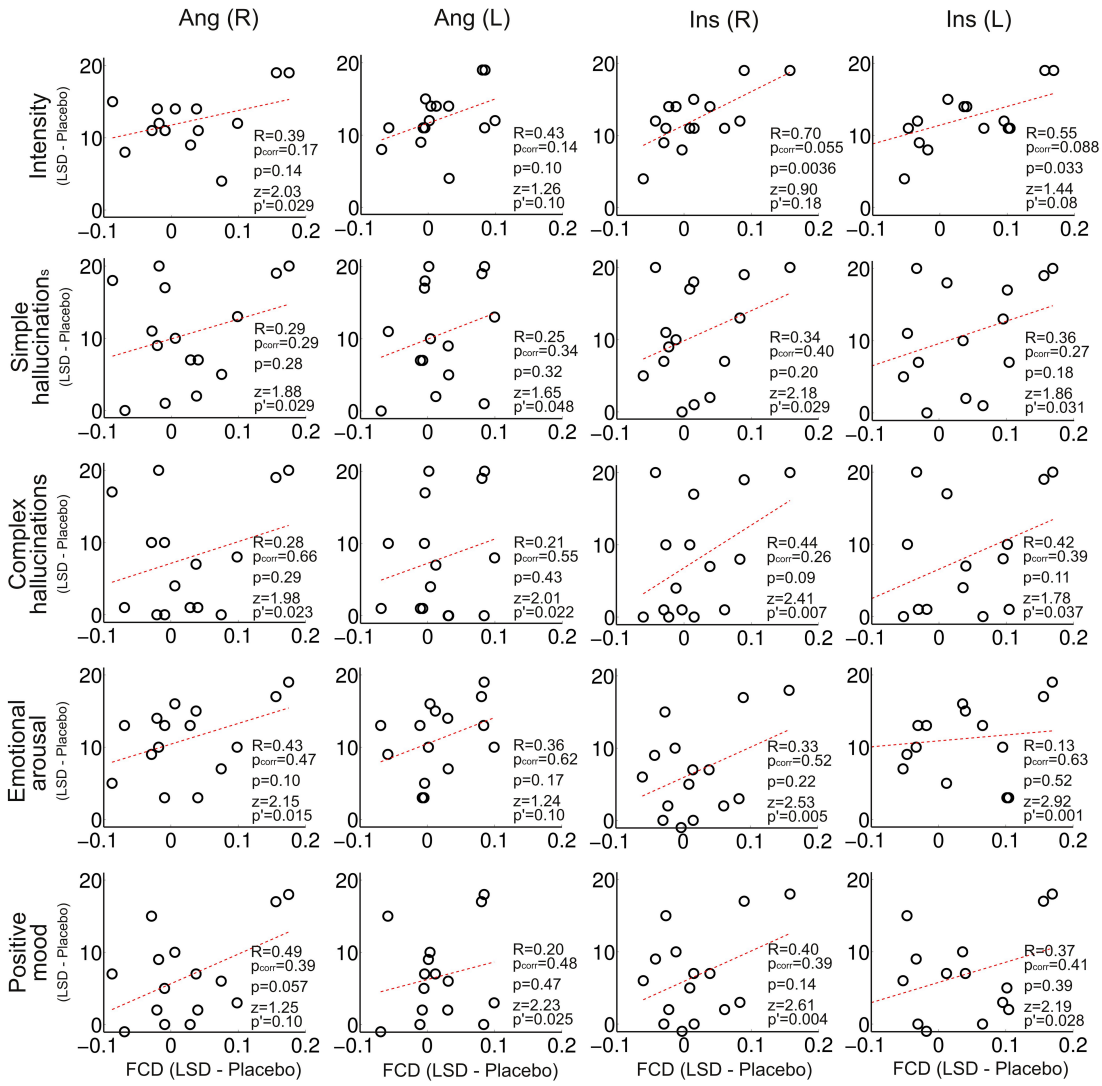

Figure S4: Scatter plots of FCD increases (LSD minus placebo) vs. VAS items: “Intensity”, “Simple hallucinations”, “Complex hallucinations”, “Emotional arousal” and “Positive mood”, for the regions presented in Figure 2B (Angular gyrus R/L and insula R/L). In the insets, the following statistics are provided. R: Pearson’s linear correlation coefficient between variables, p_{corr}: p-value for the correlation (FDR-controlled for multiple comparisons across all 401 regions in the template), p: uncorrected p-value for the correlation, z: z-values for the test of higher correlation between FCD increases and ego-dissolution vs. FCD increases and other VAS items, p’: the p-value corresponding to the z-value. These z and p-values were obtained using the following web utility: http://quantpsy.org/corrtest/corrtest2.htm.

For all except four of the comparisons we obtained p’<0.05, supporting the specificity of the correlations with ego-dissolution in this set of regions. Of those comparisons with p’>0.05, half of them corresponded to correlations with the “Intensity of the experience” item. This seems to indicate that feelings of ego-dissolution carry the most weight when participants rate the intensity of their experience, also supported by the fact that, among all VAS items, “Intensity” presented the strongest correlations with “Ego-dissolution” (Figure S2, panel C).

Supplemental Experimental Procedures

Subject recruitment and experimental design

This study was approved by the National Research Ethics Service (NRES) committee London - West London, and was conducted in accordance with the revised declaration of Helsinki (2000), the International Committee on Harmonization Good Clinical Practice guidelines and the National Health Service (NHS) Research Governance Framework. Imperial College London sponsored the research, which was conducted under a Home Office license for research with schedule 1 drugs.

Participants were recruited via word of mouth and provided written informed consent to participate after being screened for physical and mental health. The screening for physical health included electrocardiogram, routine blood tests, and urine test for recent drug use and pregnancy. A psychiatric interview was conducted with participants providing full disclosure of their drug use history. Key exclusion criteria included: < 21 years of age, personal history of diagnosed psychiatric illness, immediate family history of a psychotic disorder, an absence of previous experience with a classic psychedelic drug (e.g. LSD, mescaline, psilocybin/magic mushrooms or DMT/ayahuasca), psychedelic drug use within 6 weeks of the first scanning session, pregnancy, problematic alcohol use (i.e. > 40 units consumed per week), or a medically significant condition rendering the volunteer unsuitable for the experimental environment. Before intravenous LSD infusion participants gave a urine test for recent drug use and pregnancy, and carried out a breathalyser test for recent alcohol use.

Twenty healthy participants (4 females, mean age = 30.9±7.8 years) attended two scanning sessions in different days at 8:00 (LSD and placebo) at least two weeks apart in a balanced order, within-subjects design. Scanning days included arterial spin labeling (ASL) and fMRI followed by a MEG session. LSD (75 μg in 10 ml saline) or placebo (10 ml saline) was delivered as bolus injections over 2 minutes while participants were instructed to close their eyes and relax. Following an acclimatization period of 60 minutes inside a mock MRI scanner, three fMRI scans were conducted in the following order: eyes-closed resting state, rest while listening to music and another eyes-closed resting state session. Only results for the first resting state session (prior to music) are reported here

The intensity of subjective effects was stable for BOLD scans. Participants carried out VAS-style ratings after each scan by pressing buttons on a button-box (see next sub-section). The 11 factor altered states of consciousness (ASC) questionnaire was completed at the end of each dosing day. Here we focused on the VAS ratings, since they were specific to the time of fMRI acquisition and do not rely on retrospective evaluation of the experience, like the ASC questionnaire (moreover, it would have been impractical to have completed the ASC during scanning, as it contains 94 items, and none of them directly refers to the experience of “ego-dissolution”). In particular, we assessed correlations with the intensity of ego-dissolution experienced by the participants. All participants reported closed-eye visual hallucinations and marked changes in consciousness under LSD.

VAS items

The scale for the VAS items ranged from 0 to 20. Items were phrased as follows:

1) “Please rate the intensity of the drug effects during the last scan”, with a bottom anchor of “no effects”, a mid-point anchor of “moderately intense effects” and a top anchor of “extremely intense effects”;

2) “With eyes closed, I saw patterns and colours”, with a bottom anchor of “no more than usual” and a top anchor of “much more than usual”;

3) “With eyes closed, I saw complex visual imagery”, with the same anchors as item 2;

4) “How positive was your mood for the last scan?”, with the same anchors as item 2, plus a mid-point anchor of “somewhat more than usual”;

5) “I experienced a dissolving of my self or ego”, with the same anchors as item 2;

6) “Please rate your general level of emotional arousal for the last scan”, with a bottom anchor of “not at all emotionally aroused”, a mid-point anchor of “moderately emotionally aroused” and a top anchor of “extremely emotionally aroused”.

ASC items

As part of the ASC questionnaire the participants were asked to rate the intensity of the following items:

1) Experience of unity
2) Spiritual experience
3) Blissful state
4) Insightfulness
5) Disembodiment
6) Impaired control and cognition
7) Anxiety
8) Complex imagery
9) Elementary imagery
10) Audio-visual synesthesia
11) Changed meaning of percepts

Anatomical Scans

Imaging was performed on a 3T GE HDx system. These were 3D fast spoiled gradient echo scans in an axial orientation, with field of view = 256 × 256 × 192 and matrix = 256 × 256 × 192 to yield 1mm isotropic voxel resolution. TR/TE = 7.9/3.0ms; inversion time = 450ms; flip angle = 20°.

fMRI Data Acquisition

BOLD fMRI data was acquired in two sessions using a gradient echo planar imaging sequence, TR/TE = 2000/35ms, field-of-view = 220mm, 64 × 64 acquisition matrix, parallel acceleration factor = 2, 90° flip angle. Thirty-five oblique axial slices were acquired in an interleaved fashion, each 3.4mm thick with zero slice gap (3.4mm isotropic voxels). The length of the BOLD scan was 7:20 minutes.

fMRI data preprocessing

Resting state fMRI data was analyzed using FSL [S2], AFNI [S3], Freesurfer [S4] and ANTs [S5]. Of the total 20 subjects scanned, one subject did not complete the BOLD scans and four subjects were discarded due to high levels of head movement – as measured with framewise displacement (FD) [S6] - between LSD and placebo (difference in mean FD = 0.351±0.397).

The following preprocessing stages were performed to the remaining 15 subjects: removing the first three volumes; despiking (3dDespike, AFNI); slice time correction (3dTshift, AFNI); motion correction (3dvolreg, AFNI) by registering each volume to the volume most similar, in the least squares sense, to all others (in-house code); brain extraction (BET, FSL); rigid body registration to anatomical scans (twelve subjects with FSL's BBR, one subject with Freesurfer's bbregister and two subjects manually); non-linear registration to 2mm MNI brain (Symmetric Normalization (SyN), ANTs); scrubbing [S7] using an FD threshold of 0.4 (the mean percentage of volumes scrubbed for placebo and LSD was 0.3±0.8% and 1.8±2.4%, respectively. The maximum number of scrubbed volumes per scanning session was 7.8%). Scrubbed volumes were replaced with the mean of the surrounding volumes. Further preprocessing included spatial smoothing (FWHM) of 6mm (3dBlurInMask, AFNI); bandpass filtering between 0.01 to 0.08 Hz (3dFourier, AFNI); linear and quadratic detrending (3dDetrend, AFNI); regressing out 9 nuisance regressors: out of these 6 were motion related (3 translations, 3 rotations) and 3 were anatomical (not smoothed). The anatomical nuisance regressors were: ventricles (Freesurfer, eroded in 2mm space); draining veins (DV) (FSL's CSF minus Freesurfer's Ventricles, eroded in 1mm space); and, local white matter (WM) (FSL's WM minus Freesurfer's subcortical grey matter (GM) structures, eroded in 2mm space. AFNI's 3dLocalstat was used to calculate the mean local WM time series for each voxel (using a 25mm radius sphere centered on each voxel) [S8]

Motion

After discarding four subjects due to head motion, fifteen subjects were left for the BOLD analysis. The difference in motion for these subjects was still significant (mean FD of placebo = 0.076±0.036, mean FD of LSD = 0.12±0.05, p=0.0005). RSFC analysis is very sensitive to head motion [S7] and therefore special consideration was put to control for motion. More detail about the dedicated preprocessing steps we performed to reduce motion artifacts and other sources of noise is provided below. Despiking has been shown to improve motion correction and create more accurate FD values . The lowpass filter of 0.08 Hz has been shown to perform well in removing high frequency motion [S11]. We covaried out six motion regressors; this is because using more than six regressors (e.g., Friston's 24) is likely to be redundant and even remove real neural signal [S12]. Using anatomical regressors is also a common step to clean noise. In our pipeline instead of using global WM regressors, we used local WM which has been suggested to preform better than using the global WM [S13]. It is suggested that head movement changes RSFC results in a distance dependant matter [S6]. Therefore, as a quality control step, at the end of the preprocessing, we plotted cloud plots to look for correlation between inter-node euclidian distance and FD-RSFC correlation across subjects. In some cases in which motion is affecting the results, proximal nodes will have high FD-RSFC correlations and distal nodes will have low FD-RSFC correlations. This would result in a negative correlation between distance and FD-RSFC correlation. In our data this correlation was very close to zero for both placebo and LSD suggesting that preprocessing successfully controlled for distance-related motion artifacts.

As a final control for motion artifacts we correlated the difference in FCD values (LSD minus placebo) against the difference in FC (LSD minus placebo) across all 15 participants and the

401 regions of interest. Only 5 regions revealed a significant (uncorrected) p-value (p values = 0.0329, 0.0250, 0.0287, 0.0347, 0.0439), with none surviving correction for multiple comparisons. Furthermore, we did not observe significant FCD differences in these 5 ROI between the LSD and placebo conditions (corrected p values for the FCD comparison in the 5 ROIs: 0.1845, 0.2099, 0.1379, 0.1827, 0.0906). The same computation was performed for the time series of individual realignment parameters (three translations and three rotations), with null findings in all cases except translations along the x-axis. In this case only 3 ROIs presented significant differences between groups, but none were located among those where we observed differences in FCD.

Functional connectivity density and seed correlation

To compute the functional connectivity density (FCD) we first extracted the average BOLD signal from each of the 401 ROIs. Then, we computed the linear correlation (functional connectivity) between each one of the $(401^2 - 401)/2$ pairs of ROIs, resulting in a correlation matrix C_{ij} having in its i,j the functional connectivity between the i-th and j-th ROIs. The FCD of the k-th ROI is defined as the average of C_{ij} with respect to index j, i.e. $\frac{1}{n}\sum_{j=1}^{n} C_{kj}$ (where n equals the total number of ROIs, in this case n=401).

Seed correlation was computed by extracting the average BOLD signal from each of four masks based on significant FCD increases under LSD (frontal, parietal, precuneal and thalamic masks). Then, for all 401 ROIs we computed the linear correlation between its averaged BOLD signal and the signal from the mask, and assigned the resulting correlation value to the ROI. This resulted in a spatial map of correlations with the seed.

Modularity of functional networks

To compute the modularity of functional networks we first derived the binary adjacency matrix A_{ij} from the weighted correlation matrix C_{ij}. This was done by thresholding the correlation matrix so that $A_{ij} = 1$ if $C_{ij} > \rho$ and $A_{ij} = 0$ otherwise. The threshold ρ was selected to achieve a fixed value of link density, defined as the number of connections present in the network over the total number of possible connections (i.e. $\frac{1}{n^2}\sum_{ij=1}^{n} A_{ij}$). It is important to compare binary networks with the same link density, thus guaranteeing changes are driven by the topological re-organization of connections between conditions and not by the total number of connections. The link densities under study ranged from 0.01 to 0.5; following previous work (e.g. [S14]) the upper limit prevents the construction of excessively connected networks.

The intuition behind modules is that of a group of nodes having denser within-group connections in comparison to between-group connections (i.e. connections with other modules). The modular structure of a network can be obtained by maximizing the modularity Q, which estimates the difference between the number of intra-module links and the expected number (for the same partition) in a random network of the same size [S15]. Given a certain partition of the nodes into non-overlapping subsets, the modularity associated with this partition with this partition is defined as,

$$Q = \frac{1}{2L}\sum_{i,j} \delta(i,j)\left[A_{ij} - \frac{k_i k_j}{2L}\right]$$

The sum runs over all network nodes, L is the total number of links $\sum_{i>j}^{n} A_{ij}$, $k_i = \sum_{j=1}^{n} A_{ij}$ is the degree of the i-th node (i.e. number of links attached to the node) and $\delta(i,j) = 1$ if the i-th and

j-th nodes belong to the same subset in the partition and 0 otherwise. We computed the modularity of networks by keeping the maximal value obtained after 500 iterations of the Louvain algorithm as implemented in the Brain Connectivity Toolbox (https://sites.google.com/site/bctnet/) [S16].

Rich club coefficient

The rich club coefficient $\Phi(k)$ is computed by dividing the number of links present between all nodes with degree higher than k by the maximum possible number of links between them. The rich club coefficient is normalized by the same metric computed after degree-preserving randomization of the network. We computed $\Phi(k)$ using the algorithms provided in the Brain Connectivity Toolbox (https://sites.google.com/site/bctnet/) [S16].

Resting State Networks (RSN)

RSNs were obtained using Independent Component Analysis (ICA) on scans from the Human Connectome Project (HCP) [S17]. All of the scans were preprocessed as part of the HCP [S18]. Two BOLD resting state scans (with opposite direction of phase encoding gradient) for 35 subjects were used in this analysis. Each scan was 14:33 minute long (TR/TE=720/33.2ms, 2mm isotropic voxels). All scans were bandpassed using the same filter as our BOLD scans (0.01 to 0.08 Hz). FSL's MELODIC was used to extract the ICA components which were then visually identified [S19].

Testing the significance of the spatial overlap between networks

The overlap was determined by comparing the percentage of voxels in the networks included in the FCD/seed correlation difference maps to the same numbers obtained from 500 instances of spatial randomisation of the networks (preserving the first-order statistics of the images). Spatial randomization was performed by phase randomization on the frequency space; i.e. applying a Fast Fourier Transform to the 3D volumes, randomizing phases and then back-transforming to the spatial domain. Empirical p-values were derived from the number of instances in which the overlap with the spatially randomised networks was higher than the overlap computed using the real RSN.

Statistical testing

In all cases we compared the LSD and placebo conditions using paired t-tests.
We applied FDR to control for the rate of false positives when performing one test per ROI (n=401). This comprised the results presented in Fig. 1C, Fig. 2A, Fig. 3, Fig. 4C and Fig. S1. When the number of comparisons was smaller (e.g. one test per RSN, n=8) we used the Bonferroni correction instead. This comprised the results presented in Fig. 1D and Fig. S2.

Supplemental References

S1 Tagliazucchi E, et al. Enhanced repertoire of brain dynamical states during the psychedelic experience. Hum Brain Mapp *35* (2014):5442-5456.

S2 Smith, Stephen M., et al. Advances in functional and structural MR image analysis and implementation as FSL. Neuroimage 23 (2004): S208-S219.

S3 Cox, Robert W. AFNI: software for analysis and visualization of functional magnetic resonance neuroimages. Computers and Biomedical research 29.3 (1996): 162-173.

S4 Dale, Anders M., Bruce Fischl, and Martin I. Sereno. Cortical surface-based analysis: I. Segmentation and surface reconstruction. Neuroimage 9.2 (1999): 179-194.

S5 Avants, Brian B., Nick Tustison, and Gang Song. Advanced normalization tools (ANTS). Insight J (2009): 1-35.

S6 Power, Jonathan D., et al. Methods to detect, characterize, and remove motion artifact in resting state fMRI. Neuroimage 84 (2014): 320-341.

S7 Power, Jonathan D., et al. Spurious but systematic correlations in functional connectivity MRI networks arise from subject motion. Neuroimage 59.3 (2012): 2142-2154.

S8 Jo, Hang Joon, et al. Mapping sources of correlation in resting state FMRI, with artifact detection and removal. Neuroimage 52.2 (2010): 571-582.

S9 Wong, E. C., Buxton, R. B., Frank, L. R. (1998). Quantitative imaging of perfusion using a single subtraction (QUIPSS and QUIPSS II). Magnetic resonance in medicine, 39(5), 702-708.

S10 Buxton, R. B., Frank, L. R., Wong, E. C., Siewert, B., Warach, S., & Edelman, R. R. (1998). A general kinetic model for quantitative perfusion imaging with arterial spin labeling. Magnetic resonance in medicine, 40(3), 383-396.

S11 Satterthwaite, Theodore D., et al. An improved framework for confound regression and filtering for control of motion artifact in the preprocessing of resting-state functional connectivity data. Neuroimage 64 (2013): 240-256.

S12 Bright, Molly G., and Kevin Murphy. Is fMRI noise really noise? Resting state nuisance regressors remove variance with network structure. NeuroImage(2015).

S13 Jo, Hang Joon, et al. Effective preprocessing procedures virtually eliminate distance-dependent motion artifacts in resting state FMRI. Journal of applied mathematics 2013 (2013).

S14 Schröter, M. S., Spoormaker, V. I., Schorer, A., Wohlschläger, A., Czisch, M., Kochs, E. F, Zimmer, C., Hammer, B., Schneider, G., Jordan, D., Ilg, R. (2012). Spatiotemporal reconfiguration of large-scale brain functional networks during propofol-induced loss of consciousness. J. Neurosci. 32(37), 12832-12840.

S15 Newman, M.E., Girvan, M. (2004) Finding and evaluating community structure in networks. Phys. Rev. E 69(2), 026113.

S16 Rubinov, M., Sporns, O. (2010) Complex network measures of brain connectivity: uses and interpretations. Neuroimage 52(3), 1059-1069.

S17 Van Essen, David C., et al. The WU-Minn human connectome project: an overview. Neuroimage 80 (2013): 62-79.

S18 Glasser, Matthew F., et al. The minimal preprocessing pipelines for the Human Connectome Project. Neuroimage 80 (2013): 105-124.

S19 Beckmann, Christian F., et al. Group comparison of resting-state FMRI data using multi-subject ICA and dual regression. Neuroimage 47.Suppl 1 (2009): S148.